COMPREHENSIVE METHOD OF STUDYING AND PREDICTING THE DEFORMATION OF CERAMIC PRODUCTS DURING SINTERING

D. V. Andreev[1] and A. I. Zakharov[1]

A comprehensive method is proposed for predicting the deformation of ceramic products under their own weight (the force of gravity) during sintering. The method is based on the torsion of thin-walled tubes, finite-element modeling, a calibration process that includes tests of specimens of the material in cantilever bending, and validation of the numerical solution. The method can be used to predict the deformation of thin-walled and solid products made of materials whose rheology is based on the mechanisms of viscous and/or diffusion flow.

Keywords: ceramic products, prediction, modeling, finite-elements method, calibration, validation, deformation, creep, viscosity.

INTRODUCTION

Automated finite-element (FE) modeling is one of the modern tools now being used to design ceramic products. Such modeling makes it possible to predict the deformation of semifinished products, but their use requires an adequate rheological model of the given material and its empirical verification.

It is known that ceramic materials exhibit nonlinear viscoelastic properties during sintering [1]. Under static loading, their rheology is often represented by a mathematical model that combines an elastic spring with a damper in a series connection. Under dynamic loading, the rheology of ceramics is represented by the viscoelastic state model (Fig. 1). Whereas the deformation ε of ceramics is mainly the result of viscous flow during static loading, this need not be considered in the viscoelastic case. As regards the latter, the material's deformation can be represented as the purely viscous flow which it undergoes during a certain period of time *t* [2, 3]. Here, it is generally assumed that the deformation which ceramics experience due to sintering and the applied stresses σ are subject to the superposition principle [2] and that these materials' rheology can be modeled by a simple linear-viscous constitutive relation (Newton's law for viscous flow) [2 – 4]. It is noteworthy that the linear character of this relation is consistent with diffusion-based creep mod-

els — which also posit a linear relationship between stress and deformation rate.

Among the fine-grained ceramics whose sintering involves the participation of a liquid phase, materials of the porcelain group present the greatest challenge in terms of being able to predict their deformation. The difficulty stems from their complex variable composition and the high probability of deformation due to the presence of a large amount of the liquid phase. During sintering, a glazed porcelain semifinished product can be regarded as a three-layer material that experiences a change in it properties. The semifinished product consists of the porcelain substrate, a glaze coating, and an intermediate layer whose mechanical and other properties are appropriately anisotropic. The porcelain undergoing sintering is itself a complex micro-composite material that includes a nonuniform fluid-like material and structural units such as pores and crystalline phases [5, 6]. The ratio of the amount of matrix to the amount of structural units in the
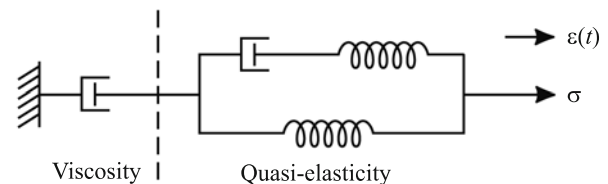

Fig. 1. Mechanical model of viscous behavior: the viscous element is series-connected to a quasi-elastic coupling composed of a damper and two elastic elements.

[1] Russian University of Chemical Engineering, Moscow, Russia.

material varies. The deformation of the semifinished product can be significantly influenced by the stresses that develop due to the different rates of contraction of the ceramic substrate and the layer of glaze. Texture, residual stresses, and density gradients are manifest to different degrees in the semifinished products, depending on the constituent material and the methods used to shape and dry it. Texture, residual stresses, and density gradients can result in warpage of the material during sintering and necessitate rejection of the finished product; nonuniform heating of the semifinished product in the furnace can also lead to rejection.

Due to the complexity of performing tests at high temperatures, rheological parameters are usually determined by means of relatively simple and accessible methods, indirect measurements, calibration algorithms, and other tools. For example, the data needed to model the deformation of porcelain tableware by the finite-elements method was obtained indirectly based on determination of the temperature dependence of Young's modulus and detailed study of the phenomenology of sintering.

The use of theoretical approaches based on equations that describe diffusional sintering, grain growth, etc. makes it possible to examine the effect of temperature gradients on shrinkage of the product without allowance for the gravitational component and friction against the refractory substrate. Generalizing makes it possible to take theoretical models developed to predict the deformation of semifinished products made of different ceramics (such as the parts of structural ceramics) and also use them to model the deformation of domestic porcelain products and sanitary ceramics [8]. Modern theoretical models can include several dozen different parameters and equations (sub-models), and the error of these models increases with the number of parameters and equations. The use of such models entails calibration of the parameters and their "manual variation." In constructing theoretical models and evaluating their parameters, modeling tools such as the Monte Carlo method and molecular dynamics are best suited for auxiliary materials with a relatively simple structure.

The calibration process generally involves subjecting geometrically simple solid specimens to high-temperature tests in tension and compression. In the tests, the longitudinal and transverse dimensions of the specimens are measured as they undergo constant or cyclic loading while being sintered. The test results are compared with data obtained from modeling performed with suitable FE-models, any necessary corrections are made to the parameters of the material model, and the modeling operation is performed again. This iterative approach maximizes the agreement that is ultimately obtained between the results. However, the loading that the specimens undergo during the tests can result in their assuming a complicated shape that is asymmetrical; quantitatively evaluating their deformation becomes more problematic in this case, and the accuracy of the evaluation depends on the method used to average the specimen's dimensions. As a rule, specimen deformation is evaluated by using dimen-

sionless parameters with a range of values from 0 to 100% [9].

The type of test just described can be used to approximately determine the bulk and shear viscosity of ceramic semifinished products. The dependence of these two properties on stress and temperature (time) in turn determines the rheological properties in complex models of the deformation and sintering of quasi-solid media. Changing from uniaxial deformation to deformation in shear (changing from Trouton viscosity to Newtonian viscosity) creates a large error for materials with a complex structure (complex rheology), since their resistance to deformation in tension may be quite different from their deformation resistance in compression [10]. Accounting for this difference is also important for the modeling operation, since either compressive strains or exclusively tensile strains may be created in semifinished products of complex shape. Moreover, loading in tension or compression does not allow the deformation which takes place under load to be determined separately from the deformation which occurs due to sintering (contraction) of the material.

The theoretical models that have been constructed to describe materials with a complex structure are appreciably less accurate than phenomenological models. Although a phenomenological model is oriented toward the specific material chosen for investigation, it may also be able to describe the rheology of an entire group of materials. To illustrate, domestic porcelain, sanitary-technical porcelain, and semi-porcelain do not differ significantly in their rheological behavior during sintering even though they differ considerably from one another in their compositions and sintering intervals. Thus, they can all be described by the same phenomenological model [6].

Various forms of specimen loading in bending and different methods based on them are usually used to perform studies of a qualitative nature. Strictly speaking, they are not suited for determining the viscosity of a material that is being sintered. Nevertheless, by allowing such materials to be examined as structural elements whose deformation is anisotropic, these methods do make it possible to test a multi-layered (composite) material under loading conditions that are similar to the conditions encountered in service. When deformation is calculated by these methods, it is customary to introduce corrections in order to account for the effect of various factors that require special attention (but are outside the scope of the problem being studied). One example would be the friction created between the edges of a product being sintered and the surface of the refractory substrate [7, 8].

Various methods based on modeling — including methods whose results are highly approximate and methods that are very accurate — are finding increasing practical use. In this article, we present a comprehensive method for modeling the deformation of complex thin-walled ceramic products during sintering. The proposed method can take the place of the approach which has traditionally been used in design. It includes an extensive series of cycles involving the

fabrication of specimens to correct the model of the semifinished product, torsional loading of thin-walled tubes [11], the use of a calibration-based method of testing of specimens in cantilever bending, validation of the numerical solution, and finite-element modeling. The main assumptions made in the modeling operation:

– the material is a continuum whose rheological behavior is described by Newton's law for viscous flow;

– the volumetric deformation of the material (the sintering rate) is independent of the stress field;

– the temperature field is uniform.

Here, we examine the use of the new method to predict the deformation of products made of biscuit (unglazed) domestic porcelain during their sintering. The material being examined is one of a group of materials that has the above-described features which are of interest from the rheological standpoint [5, 6] and for the purpose of predicting deformation in general [8]. The series of steps involved in fabricating and sintering the specimens used in the investigation correspond to the technology normally employed in making thin-walled products of biscuit porcelain. An additional step that is included is pre-sintering: heating of the specimens to 900°C at a rate of 10°C/min, holding them at the maximum temperature for 30 min, and cooling them together with the furnace. All of the specimen tests were performed during the final sintering, which was conducted in accordance with the following regime: heating to 890°C at a rate of 10°C/min, followed by heating to 1300°C at 2°C/min (for the calibration method) or to 350°C (for the validation method) and cooling together with the furnace.

CALIBRATION METHOD

The deformation of solid products can be modeled by using data obtained from tests of specimens in pure shear [11] and ignoring the effects of surface phenomena on the rheology of the material — which in the present case are negligible. However, edge effects must be taken into account in order to be able to predict the deformation of thin-walled products. Making such an accounting is a separate problem in and of itself. It is best to solve the types of problems being discussed here by calibrating the variables. Calibration is necessary to improve the accuracy of the results when dealing with complex problems that have a large number of factors and require an integral solution. In addition, calibration provides useful research data that can be used to make a detailed analysis of the reasons for deviation of the predicted results from the experimental findings.

Surface phenomena which are not accounted for are manifest to varying degrees, depending on the complexity of the specimen's shape and the technological conditions. The calibration method that is used should be able to make fine distinctions between the surface effects and the nature of the behavior of the material predicted by the model. As an empirical approach, calibration can be used to account for either

a single factor or a whole range of factors at different stages during the modeling operation. The choice here depends on the opportunities that are presented for conducting calibration experiments in each case.

Calibration entails performing additional tests and analyses and then using a parametric approach to include the results in the calculation of the FE-model. In the problem formulated here, the calibration process can be carried out by correcting experimentally obtained values of viscosity. However, it would be preferable (and, equivalently, more convenient) to do this by using an algorithm that corrects the final result.

Special attention should be given to the setup of the tests. Of the many different types of loading, we chose to subject cantilevered specimens to deformation under their own weight. Such deformation adequately simulates deformation in bending, which is the main type of loading that results in the deformation of thin-walled products during sintering. In the competing schemes that were chosen for use — methods involving two- and four-point loading of beam-shaped specimens — the deformation of the material is significantly influenced by the friction of the beam against the supports and by the longitudinal stresses which are caused by thermal expansion and contraction. Cantilever loading is preferable to two- and four-point bending in the fact that it obviates the need to account for and model the contact surfaces. On the other hand, the error connected with the fact that the given type of loading is highly sensitive to nonuniform heating of the specimen's top and bottom layers (a nonuniformity that is particularly noticeable within the temperature range in which the material undergoes rapid shrinkage [12]) should not cause the predicted deformation to deviate significantly from the actual value because the loading is auxiliary in manner.

The calibration method includes the following stages: 1) experimental studies of the deformation of the calibration specimen; 2) modeling of the deformation of that specimen by the FE method; 3) comparison and analysis of the results obtained from the modeling and the experiments; 4) application of the resulting data.

Experimental studies of the deformation of cantilevered specimens under their own weight

Cantilevered specimens in the form of beams of rectangular cross section were cut from the relatively thin walls of cylindrical semifinished products formed by slip casting and subjected to preliminary sintering.

The straightened specimens were placed in the furnace with the use of a simple fixture made of a refractory ceramic. Here, both sides of one end of each specimen were rigidly clamped in the fixture while the opposite end was left free to act as a cantilever. Refractory baffles were positioned alongside the specimens to protect them from radiation from the furnace's silicon carbide heaters and prevent overheating of their surface. The average length and width of the cantilevered parts of the specimens before the tests were 4×10^{-2}

and 1×10^{-2} m, respectively. Their thickness was within the range $(0.263 \pm 0.016) \times 10^{-2}$ m, which is associated with a confidence level of 0.95. The accuracy of the specimens' orientation in the horizontal position was checked visually as they were installed in the fixture.

The test results show that the average deflection was $(0.595 \pm 0.16) \times 10^{-2}$ m (confidence level 0.95). It should be pointed out that the specimens differed significantly in the amount of deflection they underwent even though they were all made and tested under identical conditions. This difference resulted in a wide confidence interval for the estimated deflection.

Modeling the deformation of the cantilever under its own weight

Figure 2 shows the FE-model of the cantilever that was constructed with the following initial dimensions: length 0.04000 m; thickness 0.00263 m; width 0.00600 m. The integrated model of the material of the cantilever was determined by the models (characteristics) shown below.

1. Viscous behavior that is consistent with Newton's model was determined by means of the formula $\dot{\bar{\varepsilon}} = A\bar{\sigma}$, where $\dot{\bar{\varepsilon}}$ is the equivalent deformation rate; A is a proportionality factor; $\bar{\sigma}$ is the equivalent stress [13]. The temperature dependence of the coefficient A was assigned discretely in accordance with the curve (Fig. 3) calculated from the formula $A = 1/(3\mu)$. The calculation was performed on the basis of the two temperature dependences of viscosity in pure shear μ that correspond to shear stresses of 5.2 and 82 kPa. These two dependences were determined by the application of a load during the tests. The initial rheological data was obtained in [11] by testing circular thin-walled specimens in torsion. It was shown that Newtonian flow is seen within and above the range $50 - 300$ kPA for materials in the porcelain group. Thus, the second curve makes it possible to model deformation within the entire indicated range of stress.

2. Heat-induced shrinkage was modeled by assigning the rate of bulk deformation. Its dependence on temperature was assigned discretely. Shrinkage anisotropy (deformation rate) was accounted for by using values of 1.346, 0.869, and 0.785 for the anisotropy coefficients along axes 1, 2, and 3 (thickness, width, length). These values were calculated by tripling the quotient obtained by dividing the linear deformation rate by the bulk deformation rate. The temperature dependence of bulk deformation rate (Fig. 4) was determined as the sum of the three polynomial temperature dependences of linear deformation rate corresponding to the specimens' three axes of shrinkage anisotropy in the shear tests. The linear deformation rates were calculated based on the polynomial temperature dependences of shrinkage reported in [11]. It should be mentioned that these dependences were also used in calculating the temperature dependences of viscosity.

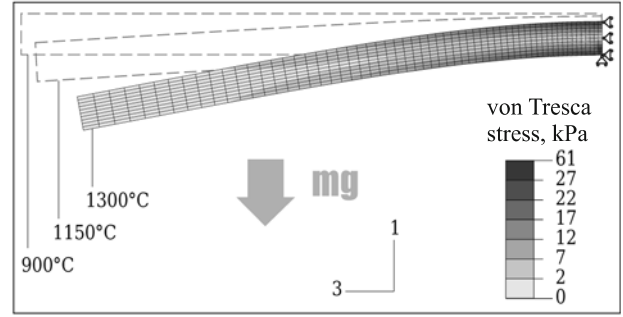3. The temperature dependence of the density of the model material was determined by assigning an initial density of 1590 kg/m³, which is equal to the experimentally determined apparent density of the material after pre-sintering at 900°C. The running value of density at each step of the FE modeling was calculated by the software on the basis of this parameter and the volume measurements.

The first computation step lasted 1 sec and the next step lasted 2999 sec, which corresponded to an increase in temperature from 900 to 1000°C; these steps were followed by 60 steps of 150 sec each, corresponding to a discrete rise in temperature from 1000 to 1300°C in 5°C increments.

The effect of gravity with a free-falling acceleration of 9.81 m/sec² was modeled by prolonging this effect from the

Fig. 2. Deformation of the FE model of the cantilever for different steps in the modeling operation and the distribution of the maximum shear stress.
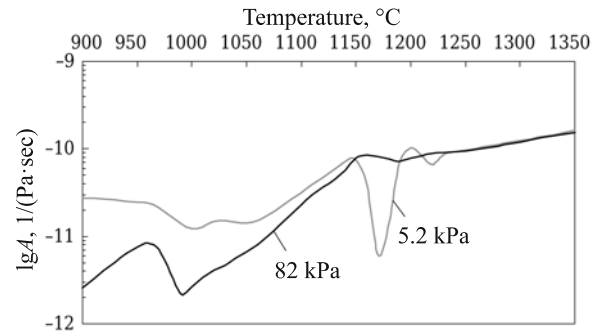

Fig. 3. Temperature dependences of lg$A$ for different shear stresses. The dependences were obtained from the results of tests of thin-walled tubes in pure shear.
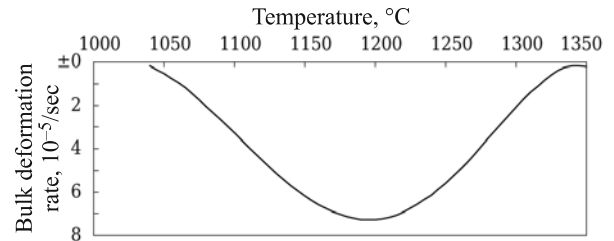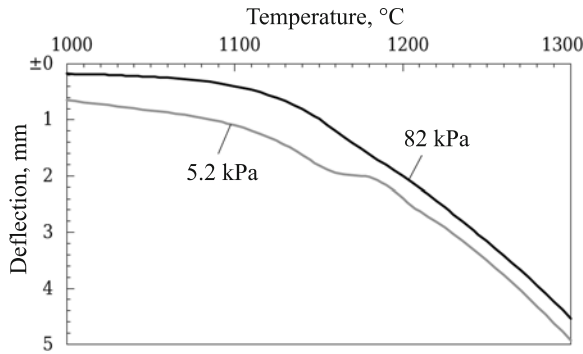

Fig. 4. Temperature dependence of bulk deformation rate obtained from the results of tests of thin-walled tubes in pure shear.

Fig. 5. Temperature dependence of the deflection of the cantilever determined by finite-element modeling with the use of data from tests performed with different shear stresses.

first step to the second step. The boundary conditions that modeled the rigid fastening of the end of the cantilever were assigned in such a way as to not place any constraints on the bulk deformation (shrinkage) of the material.

The thermal load that modeled the uniform temperature field and increased discretely over time was as follows: an average temperature of 950°C in the range from 900 to 1000°C for the first and second steps; 1005°C for the next step; a temperature that increased 5°C for each subsequent step up to the last step, which corresponded to a temperature of 1300°C.

The FE modeling determined that the deflection of the cantilever (Fig. 5) at 1300°C was 0.45×10^{-2} and 0.49×10^{-2} for the calculations performed on the basis of the viscosity data obtained experimentally with shear stresses of 82 and 5.2 kPa, respectively. The deformation of the FE-model of the cantilever and the distribution of the maximum shear stress (henceforth referred to as the von Tresca stress — see the von Tresca criterion in [13]) are shown here in frontal view (see Fig. 1). For the most part, the maximum shear stresses — which determine the deflection of the cantilever — do not exceed 27 kPa in the top and bottom layers near the base of the specimen, while these stresses are less than 3 kPa in over half the specimen's volume. A high stress concentration ranging up to 60 kPa is seen near the edge of the cantilever (the lower right corner — see Fig. 2) which rests on the horizontal support that determines the specimen's vertical position. Some of this stress concentration can be attributed to the simplifications that were made to the model. In any case, it did not have a significant effect on the amount of deflection undergone by the specimen. In light of the fact that ceramic semifinished products are more easily deformed in tension than in compression, the stresses shown in Fig. 2 are somewhat overstated in the top layer and somewhat understated in the bottom layer.

It should be mentioned that several factors which affect deformation were deliberately not modeled for the calibration process. Specifically, we ignored edge effects (high concentrations of microcracks, atmosphere-induced changes in the composition of the surface layers, consequent changes in the rheological properties of the material, etc.) that "thin" the material at the boundaries of the specimen. Thus, the deflection of the cantilever determined by FE modeling is expected to be less than the actual deflection.

To determine the effect of shrinkage on the d8 of the cantilever, we performed an additional variant of FE modeling in which we ignored the change in volume. The results showed that the effect of shrinkage (with allowance for anisotropy) on deflection is negligible. Thus, this factor need not be modeled at the given stage of the investigation.

**Comparison of the results of the modeling
and the experiments**

The relative errors of the modeling results were 24 and 18% respectively for calculations performed on the basis of viscosity data obtained experimentally with values of 82 and 5.2 kPa for the stress in pure shear. Considering the 15 – 17 kPa range for the deflection-determining maximum shear stresses (Fig. 2) and the complex dependence of viscosity on stress, it would be best to simplify the formulation of the problem by taking the average deviation of 21% as the calibration coefficient E_{cant} that is used to correct subsequent results of the modeling operation. The coefficient E_{cant} reflects the extent to which edge effects influence the deformation of the cantilever under its own weight. Expressing this coefficient in a more general form as E_f, its value depends locally on the character of the loading of the semifinished product's structural elements and should increase with an increase in the shape factor f — which is equal to the ratio of the surface area of a given structural element to its volume. The coefficient E_f can be assumed to be directly proportional to the shape factor f:

$$E_f = K_{edge},$$

where the proportionality factor K_{edge} reflects the extent to which edge effects influence the rheology of the material for the given environmental and loading conditions.

For the material of products made in the factory, these conditions usually differ from the conditions which exist in laboratory tests of specimens. If the lab tests are set up in such a way that edge effects or the shape of the material have almost no effect on its rheology, then the value of K_{edge} calculated for factory conditions will be an absolute value. Such conditions correspond exactly to the deformation in pure shear that results from the torsion of a thin-walled ring of certain dimensions [11]. Thus, in the modeling operation the coefficient K_{edge} becomes a calibration parameter that is freed of its dependence on the shape of the specimen (a rectangular cantilever in our case) by the use of the shape factor f. Although the latter cannot always be calculated manually, it can be computed by FE modeling for products of almost any shape.

We subsequently found K_{edge} on the basis of the above-calculated quantity E_{cant} and replacement of the volume V and surface area S by the corresponding average dimensions of the cantilever:

$$K_{edge} = \frac{E_{cant}}{f} = \frac{VE_{cant}}{f}$$

$$= \frac{0.04 \times 0.01 \times 0.0026 \times 0.21}{2 \times 0.04 \times 0.01 + 2 \times 0.04 \times 0.026 + 0.01 \times 0.0026} = 2.1 \times 10^{-4} \text{ m.}$$

Use of the resulting value of K_{edge} in calculating the deformation thus makes it possible to change over from pure shear to loading conditions in which flexural deformation is dominant (there is no change in the sintering conditions), since the shape factor f accounts for changes in the shape of a given structural element. One example might be a change in the thickness of the wall of the semifinished product.

VALIDATION METHOD

Validative evaluation is needed to confirm that the method of prediction which is being used has the degree of reliability required for practical purposes. To perform such an evaluation, predictions are made when the problem is formulated in such a way that the features of the object being modeled correspond to its actual features as closely as possible. The predictions are then compared with experimental results. It is best to carry out the validation process on the basis of a model formulation in which the dimensions of the semifinished product are reduced to a minimum by assigning compensating boundary conditions. In such a formulation, a complex object (i.e. the shape of the actual product and its stress field) is replaced by a representative object which is of relatively simple shape and is loaded by a relatively simple scheme but has the same local structural features as the complex object. Thus, the deformation of the representative object will adequately reflect the deformation behavior of the product that is being designed. For example, the representative object for a massive ceramic insulator that is deformed under its own weight during sintering might be a small solid cylinder of small mass (which is taken as zero for the FE-model) that is placed on a substrate with a weight applied to its top surface. To predict the deformation of more complicated ceramic products, the representative object should realize different types of stress state; the shape of the object chosen in [14] was obtained by "extruding" an inverted T-shaped piece. In addition to visual inspection, in this case the results are evaluated by using specific dimensional or dimensionless parameters of the object. It should be mentioned that the experiments used for the validation process cannot be set up in the same way as the experiments that are used to calibrate the parameters of the model.

When determining a representative object for composite materials, it is necessary to account for anisotropy, nonlinear rheologic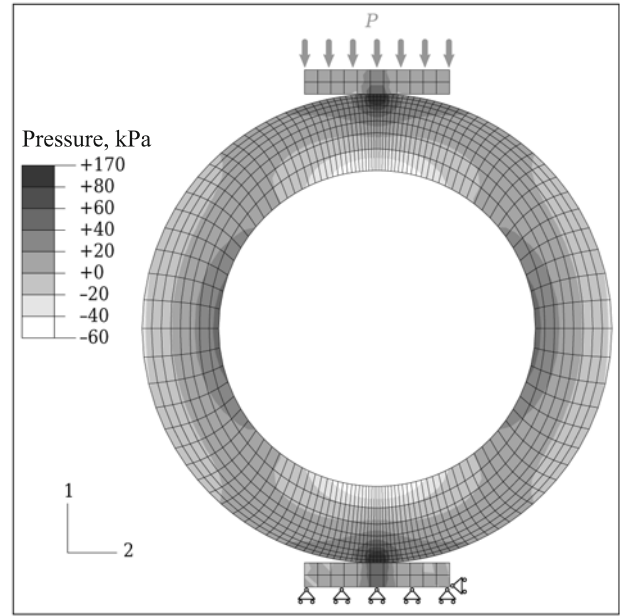al behavior, and other factors. Since most thin-walled ceramic products are made by slip casting or rolling, the representative object should account for the rheological-properties anisotropy that is characteristic of the corresponding semifinished products due to the anisotropy of their structure. Since bending is the predominant type of deformation that thin-walled products undergo, the representative volume that is used both for calibration and for validation should be a specimen whose behavior is determined mainly either by bending moments resulting from the specimen's own weight or by an externally applied mechanical load.

In this investigation, we chose a ring from among a group of shapes of varying degrees of complexity. The ring was chosen because it is the optimum shape for conducting quick lab tests; it is highly symmetrical and is well-represented by frontal views, which is convenient for modeling (Fig. 6) and for photographing the changes in its shape (Fig. 7a and Fig. 8a). A ring shape is simple for forming by slip casting, and it is resistant to defects and distortions that might be caused by the shaping and drying operations (such defects and distortions were not examined in this investigation).

The specimen must be uniformly heated on all sides during the tests. To do so, the dimensions of the specimen should be chosen so that they are significantly smaller than the dimensions of the working volume of the furnace and the specimen surface should be protected from direct radiation from the heating elements. However, the choice of dimensions for the specimen is constrained less by the furnace's working volume that it is by the dimensions of the viewing window. The viewing window must be large enough to allow the front of the specimen to be photographed by the camera
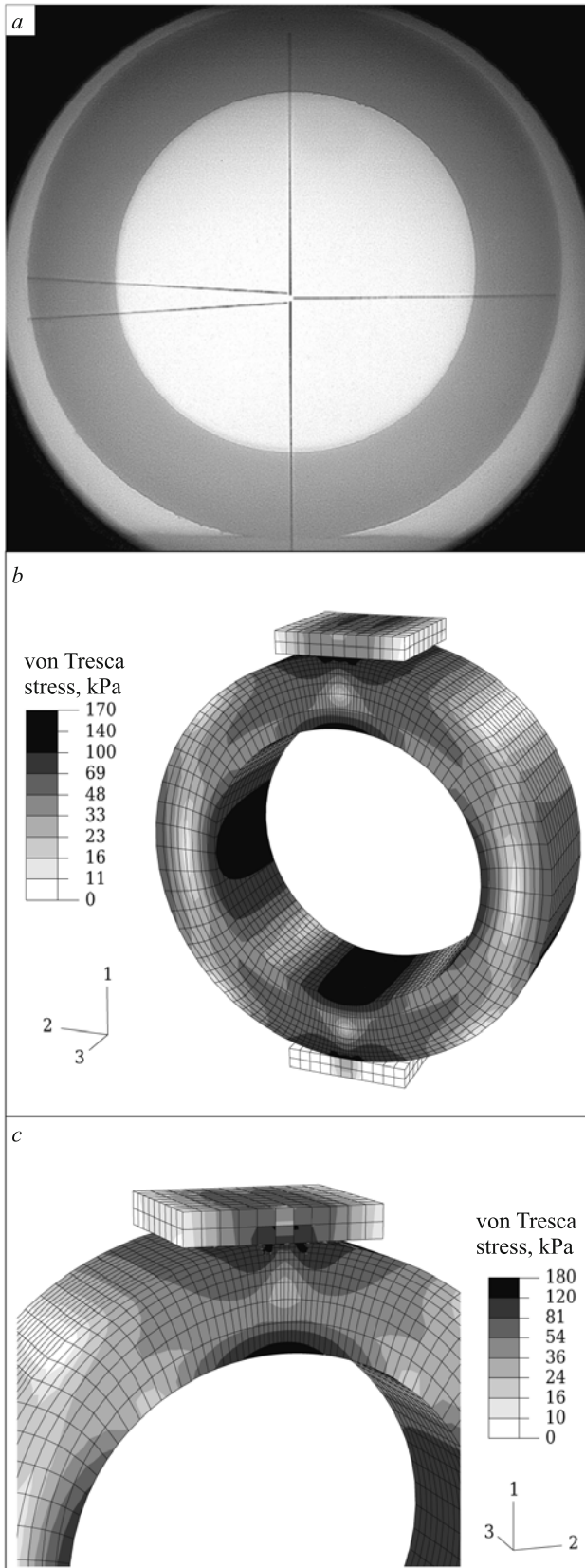

Fig. 6. The ring model at the computation step corresponding to a temperature of 900°C. The figure shows the boundary conditions and the pressure distribution from the applied load P.

Fig. 7. The ring specimen at 900°C and its model at the corresponding computation step: *a*) photograph of the front of the specimen during the test; *b*, *c*) distribution of the maximum shear stress at the end and in the transverse plane of symmetry, respectively.

that is used. The window's dimensions also depend on the distance between it and the location of the specimen in the furnace. As a result, the specimen cannot be any larger than several centimeters when a standard lab furnace is being used. In the case of specimens of this size, the stresses created by the specimen's own weight during sintering may turn out to be below the range that is of interest for the purposes of the test. However, this problem can be circumvented by the application of an external load (see Fig. 6).

**Experimental studies of the deformation
of rings under an applied load**

The conditions that exist during the different stages involved in making the ring-shaped specimens were the same as for the specimens used in torsion tests. Also, the tubular semifinished product was cast in the same mold that is used to form the working parts of the specimens used for torsion [11]. The pre-sintered tube was cut into three specimens in the form of rings. After straightening of the ends, the average dimensions of the test specimens were as follows: height along the axis 1.127×10^{-2} m; outside and inside diameters 0.975×10^{-2} and 0.657×10^{-2} m, respectively (wall-thickness 0.318×10^{-2} m). The specimens were placed near the far wall of the furnace chamber on a flat refractory stand. The specimens were located the same distance from one another on the stand and were covered by a refractory panel in the form of a equilateral triangle and a corundum-filled crucible to act as the load.

A load of $108.7g$ was applied to the ring, which ensured that the resulting stresses corresponded to the range of stresses that develop in the wall of the semifinished product under its own weight during processing. The test regime was the same as the regime employed in studying viscosity. One of the test specimens was oriented opposite the direction of the viewing window. Its deformation was recorded with a cathetometer equipped with a camera that was attached to a computer. The contours of the ring were distorted in the photographs due to the "floating image" effect caused by the temperature gradient between the flows of heated air around the specimen and the objective lens of the cathetometer. To compensate for the distortions, we took a series of photographs 10 sec apart and photographed several series 30 – 60 sec apart. The contours of the images obtained in each series were then averaged into a single final photograph by means of the program "RgiStax 4," which is designed to automatically improve the resolution of photographs that are taken automatically. These procedures were followed to ultimately obtain a series of pictures that showed the change in the shape of the specimens during tests in which they were deformed every 30 – 60 sec (the first and last photographs are shown in Fig. 7*a* and Fig. 8*a*, respectively).

Modeling the deformation of two rings in transverse compression

The modeling of the rings' deformation in transverse compression was done in a manner similar to the above-described modeling of the deformation of a cantilever under its own weight. Thus, we will discuss only the differences in the setup of the tests. To shorten the computing time required for the modeling, the problem was solved for the symmetrical part of the modeled system intercepted by the transverse plane of symmetry of the ring. The FE-model was constructed so that its height was 0.5635×10^{-2} m along the axis of symmetry (axis 3). The remaining dimensions were equal to the average dimensions of the experimental specimens. The top and bottom were modeled by provisional elements made of an ideally elastic material.

The orientation of the properties anisotropy of the material was established in a suitable cylindrical coordinate system. The temperature dependence of the coefficient A was assigned in accordance with the curve (see Fig. 3) that corresponded to a shear stress of 82 kPa. A uniform temperature field with 5°C increments in temperature was established over the range 1000 – 1350°C (steps 3 – 72) and the number of computation steps was increased accordingly.

The pressure on the outside surface of the top panel (see Fig. 6) corresponded to the force of gravity from the load applied to one ring. The top panel was prevented from moving horizontally and the bottom panel was kept from moving in any direction. In addition, the surface of the model that corresponded to the transverse plane of symmetry of the ring was kept from moving along the normal. The contact interaction of the ring with the top panel (see Fig. 6) and bottom panel was modeled with a value of 0.3 for the coefficient of external friction.

Comparison of the results

Computer visualization of the results of the modeling show complete qualitative agreement with the experimental data: comparison of the silhouette of the inside radius of the specimen that was photographed and the contour of the inside radius of the model in the end plane showed that there were no differences (see Fig. 8a); the below-mentioned distortions of the FE-model were fully consistent with the deformed shape of the specimens after the experiments. As might have been expected, however, there was significant scatter of the specimens' deformation. Despite this, the character of the deformation was the same in both cases.

A ring-shaped specimen loaded with a transverse force undergoes flexural deformation and is thus characterized by the presence of substantial compressive and tensile forces (Fig. 6). The highest (in absolute value) compressive and tensile stresses in the specimens in our investigation were in the vertical axis of symmetry and reached 170 and 60 kPa, respectively.
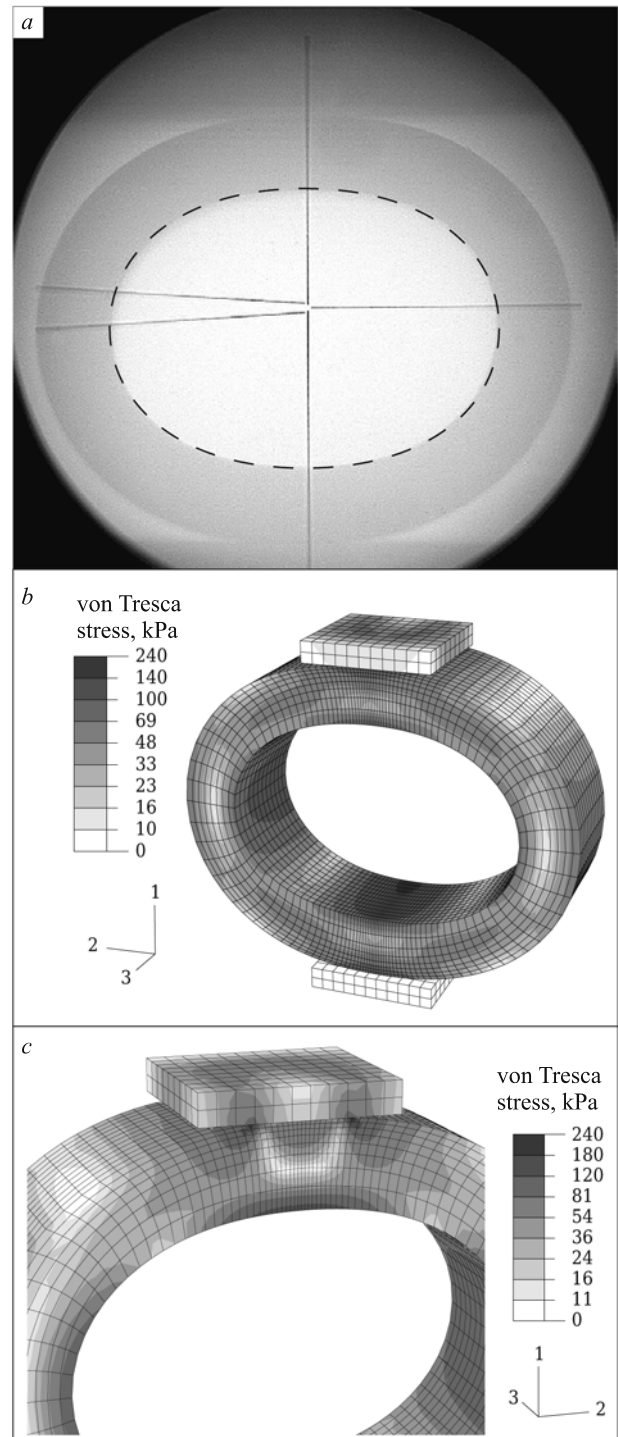

Fig. 8. Comparison of the ring specimen at 1350°C and its model at the corresponding computation step: *a*) frontal view of the specimen during the test and the contour of the model (dashed line); *b, c*) distribution of the maximum shear stress at the end and in the transverse plane of symmetry, respectively.

On the whole, the pressure distribution corresponded to a von Tresca stress field, i.e. the ratio of the respective quantities did not change over the volume of the specimen. The
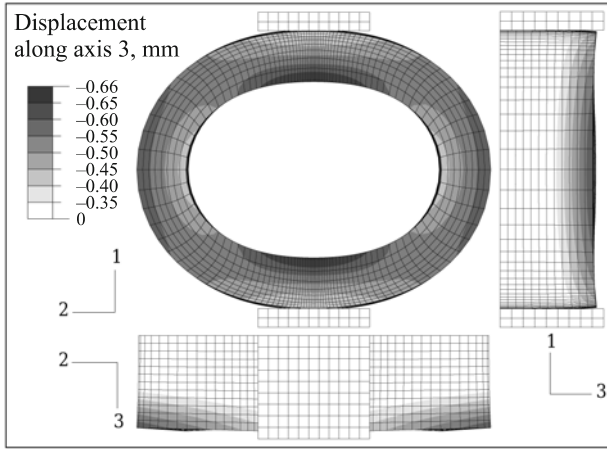
Fig. 9. Deformation of the ring specimen in three projections at the computation step corresponding to a temperature of 1350°C. The figure shows the distribution of the longitudinal displacements (along axis 3).
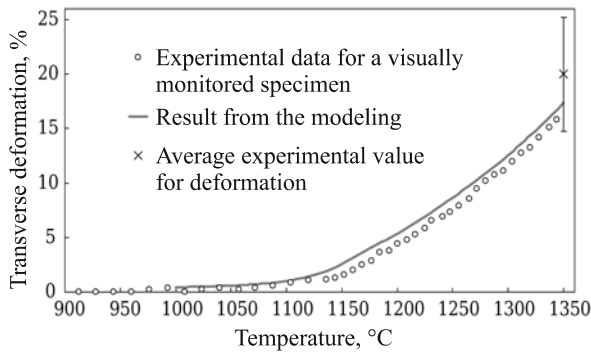

Fig. 10. Temperature dependences of the transverse deformation of the ring specimen.

stress range changed from zero to 180 kPa at the beginning of deformation and increased to 240 kPa by the end of deformation. The critical stress range in the layers (regions) of the ring that underwent intensive deformation was 70 – 140 kPa. It should be noted that this range corresponded to the shear stress at which the flow curve was obtained in the modeling operation. An increase in deformation was accompanied by an increase in the transverse (along axis 2) dimension of the contact region and the von Tresca stresses at the boundaries of the contacts. These stresses increased as a result of the increase in bulk deformation and the restraining force from external friction. Additional FE calculations were performed with the use of different values for the external friction coefficient. The results showed that the effect of the stresses associated with internal friction (the friction coefficient) on total deformation is negligible, despite their high peak values.

The stress gradient increases toward the transverse plane of the ring's cross section due to distortion of its shape as a result of longitudinal strains (along axis 3). The distortions of

the ring turned out to be significant (Fig. 9), and there were characteristic regions in which the ring was warped. Compressive forces pushed the end surfaces outward, while the region subjected to tensile forces contracted. As a result, the initially flat ends of the specimen formed a concave surface. The greatest longitudinal deformation was seen in the ring's horizontal plane of symmetry (with the end surface locally inclined toward the ring's exterior) and its longitudinal-vertical plane of symmetry (with an inward inclination). Thus, the deformation of the specimen led to ovalization of its originally circular form. Here, ovalization progressed faster near the end surfaces than near the transverse plane of symmetry.

The modeling results and the experimental results were compared quantitatively by using the function $D(w,h)$, which determines the percentage deformation of the ring:

$$D = \frac{w-h}{w+h} \times 100\%,$$

where w and h respectively are the lengths of the horizontal and vertical axes of the oval in the end plane of the inscribed circle of the original ring.

This function is convenient to use because it expresses the percentage deformation of the ring independently of its shrinkage (the dimensional scale) and accounts for the character of its deformation in transverse compression in such a way that the values of strain end up in a range extending from zero (in the absence of deformation) to 100% (when the top and bottom surfaces of the ring's inner wall end up being in contact with one another).

The graphical data on the increase in the percentage deformation of the ring during sintering shows (Fig. 10) that the strains obtained by modeling and from experimental data based on measurements of the ring's geometry in the photographs were smaller than the final strain found by averaging the results for three specimens after sintering. This difference can be attributed to the fact that the modeling was performed without allowance for edge effects, as well as the fact that the temperature to which the specimen that was photographed was heated was lower than the average specimen temperature because it was closer to the furnace's viewing window. Thus, at 1350°C, $D = (20 \pm 5)\%$ with a confidence level of 0.80 for the experiments, while $D = 17.4\%$ with a relative deviation of 13% for the FE modeling.

To incorporate calibration data that accounts for edge effects into the modeling results, we found the shape factor f for a ring-shaped specimen

$$f = \frac{S}{V} = \frac{1.48 \times 10^{-3}}{1.83 \times 10^{-6}} = 807 \, \text{m}^{-1}$$

and the calibration coefficient E_f

$$E_f = f K_{\text{edge}} = 807 \cdot 2.1 \times 10^{-4} = 0.17.$$

Thus, the deformation of the ring calculated by modeling with allowance for the calibration coefficient exceeded the deformation obtained in the experiments. The relative error here was 4.7%. The higher value obtained for the modeled deformation of the ring was due mainly to a deficiency in the experimental part of the investigation. Specifically, it was due to the above-mentioned difference between temperature conditions in the calibration experiments and the temperature conditions in the validation experiments.

CONCLUSION

The method described above makes it possible to predict the deformation of ceramic products under their own weight during sintering. The order of magnitude of the results' accuracy is satisfactory most practical applications. The method is based on procedures, equipment, and software that are readily accessible for laboratory research. The solutions found to problems by the method are quite simple and do not require a high degree of qualification in applied mechanics, programming, or other fields. The method is well-suited for materials whose rheology is based on a directly proportional dependence of strain rate on stress, i.e. on the mechanisms of viscous flow, diffusional flow, and so forth.

A procedure was found for calibrating calculated data in order to be able to account for specific features of the deformation of products of different shapes under specific conditions. The calibration procedure is especially useful for thin-walled semifinished products but is not needed for massive solid products.

REFERENCES

1. V. S. Bakunov, A. V. Belyakov, E. S. Lukin, and U. Sh. Shayakhmetov, Oxide Ceramics: Sintering and Creep [in Russian], RKhTU im. D. I. Mendeleeva, Moscow (2007).
2. R. K. Bordia and G. W. Scherer, "On constrained sintering. I. Constitutive model for a sintering body," *Acta Metall.*, **36**(9), 2393 – 2397 (1988).
3. P. Z. Cai, G. L. Messing, and D. J. Green, "Determination of the mechanical response of sintering compacts by cyclic loading dilatometry," *J. Am. Ceram. Soc.*, **80**(2), 445 – 452 (1997).
4. O. Gillia, D. Josserrond, and D. Bouvard, "Viscosity of WC-Co compacts during sintering," *Acta Mater.*, No. 49, 1413 – 1420 (2001).
5. F. Porte, R. Brydson, B. Rand, et al., "Creep viscosity of vitreous china," *J. Am. Ceram. Soc.*, **87**(5), 923 – 928 (2004).
6. D. V. Andreev and A. I. Zakharov, "Structure and rheology of semivitreous porcelain during kilning," *Glass and Ceram.*, **68**(9/10), 330 – 336 (2012).
7. J. M. Gaillard, J. C. Gault, and P. Petrault, "Prediction of tableware deformations using a finite elements analysis and the measurements of physical parameters in process conditions," in: Ceramics Today — Tomorrow's Ceramics (1991), pp. 333 – 341.
8. T. Kraft, "Simulation des Brennprozesses bei der Herstellung von Gebrauchskeramiken," *Keramische Zeitschrift*, **54**, 374 – 381 (2002).
9. E. A. Olevsky, R. M. German, and A. Upadhyaya, "Effect of gravity on dimensional change during sintering, II. Shape distortion," "*Acta Mater.*, No. 48, 1167 – 1180 (2000).
10. V.-P. P. Yakushka, Features of the Creep of Ceramics and Refractories during Different Types of Loading. Author's Abstract of Engineering Sciences Candidate Dissertation. Kaunas (1983).
11. D. V. Andreev and A. I. Zakharov, "Study of the rheology of sintered glass ceramic materials by the torsion of thin-walled tubes," *Refractories and Industrial Ceram.*, **53**(1), 31 – 39 (2012).
12. D. V. Andreev, A. I. Zakharov, and O. M. Kolesnikova, "Study of the deformation behavior of porcelain during sintering by the cantilevered-specimen method," Proc. Conf. "Advances in Chemistry and Chemical Engineering. Vol. XXII, RKhTU im. D. I. Mendeleeva, Moscow (2008), No. 7 (87), pp. 47 – 49.
13. J. Maize, Theory and Problems of Continuum Mechanics [Russian translation], Mir, Moscow (1974).
14. D. C. Blain, R. M. German, and S. Park, "Computer modeling of distortion and densification during LPS of high-performance materials," [electronic resource]. Web address: http:/www.cavs.msstate.edu/publications/2005-24.pdf (posting date 09.04.2010).